Game theoretical framework for bicycle operations

A multi-strategy framework

Hoogendoorn, Serge; Gavriilidou, Alexandra; Daamen, Winnie; Duives, Dorine

DOI
10.1016/j.trc.2021.103175

Publication date
2021

Document Version
Final published version

Published in
Transportation Research Part C: Emerging Technologies

Transportation Research Part C 128 (2021) 103175

Contents lists available at ScienceDirect

Transportation Research Part C

journal homepage: www.elsevier.com/locate/trc

Game theoretical framework for bicycle operations: A multi-strategy framework ☆

Serge Hoogendoorn *, Alexandra Gavriilidou, Winnie Daamen, Dorine Duives

Transport & Planning Department of the Delft University of Technology, Netherlands

A B S T R A C T

This paper presents a novel microscopic modelling framework for bicycle flow operations. The modelling principles are based on similar principles successfully applied in our previous work on pedestrian and vessel flow. The main contributions of the paper are in the extension towards modelling cyclists that has not been proposed in literature before, and in the insights gained by simulation with the model using different scenarios, showing how the model outcomes depend on the modelling choices and parameters.

The generalisation entails two major changes compared to our previous pedestrian model. First of all, the model does justice to the kinematics of cyclists. Contrary to pedestrians, cyclist are more restricted in their movement. The model approximates these restrictions by considering speed and movement direction and changes therein. Secondly, the model includes different strategies (cooperative, zero-acceleration, demon opponent) in its underlying game-theoretical framework, and allows including traffic rules. This allows us to model different attitudes towards risk representing different types of cyclists.

The (qualitative) insights gained by application of the model pertain to one-on-one interactions between cyclists and the impact of the strategy assumptions and parameter choices on those interactions as well as on the collective phenomena that occur in the cyclist flow and their sensitivity to parameters (reflecting the extent of the prediction horizon, the level of anisotropy, and the relative importance of keeping the desired path). With respect to the collective phenomena, we look at efficiency and self-organised patterns.

We conclude that the model acts in a plausible manner. While we do not aim to show empirical validity, we see that the qualitative behaviour of one-on-one interactions is plausible if compared to experimental or field data. We also observe plausible collective patterns, including forms of self-organisation under specific parameter settings. The latter is not trivial given the fundamental differences in bicycle and pedestrian flow.

1. Introduction

The field of bicycle flow simulation is by far not as mature as its vehicular or pedestrian flow counterpart. For one, this is because the field is relatively young, and limited data on bicycle flow operations have been broadly available. Furthermore, bicycle flow operations are much more complex than vehicle flows. This is not only due to the fact that a bicycle flow is two-dimensional and not lane-based, while vehicular flows are by and large one-dimensional, but also since bicycle flow dynamics operations (operational physical and operational mental levels) and tactical choice (route choice) levels are much more interwoven (Gavriilidou et al., 2019a).

The mathematical formalisation of cyclist behaviour and the interactions between cyclists are an essential element of any microscopic simulation model. However, few models have been put forward that capture the behaviour of cyclists realistically, while at the same time yielding valid macroscopic flow characteristics.

In this paper, we further our game-theoretical framework by first of all ensuring that we respect bicycle kinematics (referred to the operational physical level in Gavriilidou et al. (2019a)), and second of all including different interaction styles or strategies between the cyclists. In line with our previous work, we use the concept of predicted *effort minimisation*, where effort is defined

☆ This article belongs to the Virtual Special Issue on IG005584: VSI:ISTTT24.

* Corresponding author.
E-mail address: s.p.hoogendoorn@tudelft.nl (S. Hoogendoorn).

https://doi.org/10.1016/j.trc.2021.103175
Received 27 December 2020; Received in revised form 19 April 2021; Accepted 20 April 2021
Available online 25 May 2021

as a combination of components reflecting sources that result in (increased) effort or cost. In previous work (Gavriilidou et al., 2019a), we hypothesised that in determining an action, a cyclist assumes that the other cyclists do not change their course or speed. In contrast, the modelling approach presented here allows assuming that the interacting cyclists are, at least to an extent, aware of the strategy of the others. The proposed framework thereby allows modelling different cooperation strategies (e.g. cooperative interactions, non-cooperative interactions, and even hostile interactions).

At the same time, the novel model is more generic in terms of the parameters, processes, and traffic rules it can include than the previous work presented in Gavriilidou et al. (2017) (e.g. prediction, anisotropy). For instance, we include a prediction horizon that is used by a cyclist to make decisions anticipating changes in the situation. We also include (levels of) anisotropy in the model specification, and indicate how to include traffic rules (e.g. cyclist from the right have right-of-way, or overtaking on the left).

Using the resulting model specification enables investigating the impact of the type of cooperation between cyclists in varying interaction situations, the impact of model parameters on flow dynamics and self-organisation, and so forth, which are presented in this paper as well.

The contributions of the paper are of a theoretical nature. Next to presenting a novel model, we analyse the outcomes of the model in a qualitative way. This provides insight into how phenomena we see in the model results depend on behavioural assumptions and parameters (e.g. when do we see self-organisation occurring and when does it fail). The paper is outlined as follows: Section 2 provides a short overview of the relevant state-of-the-art. Section 3 presents the main assumptions underlying the model formalisation. Section 4 describes the mathematical formation of the model, while Sections 5 and 6 present simulation outcomes and show the impacts of the various parameters and strategies incorporated in the model. We end with conclusions and future work (Section 7).

2. State-of-the-art in microscopic bicycle flow modelling

In this section, we present an overview of the few microscopic models dedicated to modelling cyclist traffic operations.

The first microscopic models for cyclist operations used modelling paradigms developed for cars. One example are the Cellular Automata models, whose parameters have been adjusted to capture the smaller size and lower speeds of bicycles compared to cars (Mallikarjuna and Rao, 2009; Yao et al., 2009; Vasic and Ruskin, 2012). However, the rules that determine movements between cells have not been modified to represent cycling behaviour and interactions. In a lane-based, one-dimensional flow, a bicycle-following model has been derived and calibrated using empirical cyclist data (Andresen et al., 2013), while Zhao and Zhang (2017) showed that a unified following model can be applied to cars, pedestrians and cyclists and produce realistic macroscopic characteristics given proper scaling of the parameters. Despite this finding, single file bicycle flow is generally not representative of cyclist movements on cycling infrastructure. Due to the lack of lanes, identifying cyclist overtaking manoeuvres is not trivial, but requires specific thresholds to be differentiated from a following movement (Mohammed et al., 2019).

Apart from following and overtaking, there are more situations that a microscopic cyclist flow model should cover. These relate to the individual bicycle movement, but also to encounters with traffic participants from other directions. In Ma and Luo (2016), the acceleration process of cyclists using naturalistic data is modelled; Li et al. (2011), Liang et al. (2012), Huang et al. (2017) developed social force models that consider repulsive forces from obstacles and other traffic users, as well as an ellipse representation of the bicycle. In Gavriilidou et al. (2019a) a two-layer framework is proposed to model operational cycling behaviour using discrete choice theory and is demonstrated on bicycle interactions while forming a queue upstream of a traffic signal.

The shortcoming of all these studies is that they ignore non-verbal – but also verbal – communication between cyclists. Eye contact is crucial when cycling and visual cues indicate the intention of the cyclist in an encounter. Using those, cyclists can adopt different strategies in their interactions that cannot be captured by the existing models. Game theoretical approaches, on the other hand, can capture this, as the behaviour of the different agents depends on the strategies that they are assumed to adopt, like cooperating or not. The present paper aims to fill this gap by extending on the game theoretical model presented in Gavriilidou et al. (2017).

3. Theoretical assumptions and justification

Let us briefly describe the main assumptions regarding the behaviour of the cyclist. These will form the basis for the mathematical formulation presented in the next section.

1. The cyclist aims to optimise her behaviour (in terms of speed and direction), given the – possibly limited – knowledge of the system state and dynamics.
2. The cyclist monitors (changes in) the system state and reconsiders her control actions accordingly (receding horizon approach) at discrete, but *not necessarily equidistant*, time instants t_k. The cyclist can thus be perceived as a discrete-time feedback-oriented controller.
3. The cyclist anticipates on the behaviour of other cyclists by predicting their behaviour according to non-co-operative or co-operative strategies.
4. The cyclist is aware of the limitations of her predictions, and as a result discounts the costs of her actions over time and space.
5. The cyclist minimises the predicted discounted costs resulting from: (a) straying from the planned speed and direction); (b) the vicinity of other cyclists and obstacles, and; (c) applying control (acceleration, changing direction).

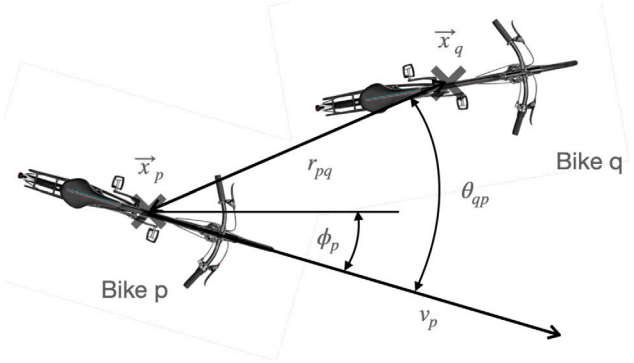

Fig. 1. Model variables including the position $\vec{x}$, speed v, direction ψ, and angle to opponent bicycle θ.

One of the key assumptions within this modelling framework is that the cyclists are hypothesised to make optimal decisions: they optimise *subjective* cost or effort (assumption 1). The *principle of least effort* is a well known and often used modelling paradigm for human behaviour. Cost can reflect many subjective factors, and has turned out to be a sufficiently generic starting principle for many mathematical rigorous modelling approaches. This behavioural assumption is grounded in the idea that experience and knowledge have skilled the cyclists in performing their tasks efficiently, and hence the assumption of optimal behaviour is deemed justified, even if choices are not consciously made. Empirical validation for both pedestrians and cyclists can be found in Robin et al. (2009) and Gavriilidou et al. (2021) respectively.

In Hoogendoorn et al. (2011) it is shown that even in continuous time tasks (in this case, car-following), decision making is often discrete in time or event-based (assumption 2). Even if this would not be the case, the assumption is generic in the sense that the inter-decision times $t_k - t_{k-1}$ can be very small (and equidistant).

Assumption 3 is well established for pedestrians (Hoogendoorn and Bovy, 2003), and is assumed here to hold for cyclists as well. Some evidence has been found in the controlled experiments described in Gavriilidou et al. (2019b), but further research on this assumption would be required to directly (or indirectly) test this hypothesis. Moreover, in Gavriilidou et al. (2017) it was observed that without including anticipation, responses appear to occur too late compared to what can be observed in reality (Yuan et al., 2018), showing the need for including it in the modelling. Also assumption 4 has been established for pedestrian flows, which we will use as a justification for including it as a basis for our cycling model.

Assumption 5 is proposed here to derive the model. The framework is however generic and allows for other cost attributes if needed.

Let us also note that the optimisation can include limitations of the cyclist in terms of observation errors, information processing and internal state estimation, as well as processing times and reaction times. Although these will not be discussed in detail in this paper, their inclusion in the proposed framework can be achieved in a relatively straightforward manner.

4. Model specification

This section describes the model specification based on the theoretical assumptions presented in the preceding section. Fig. 1 shows some of the key variables used in the model.

4.1. Bicycle dynamics modelling

The kinematics of bicycles have received quite some attention in (mechanical) research (e.g. to study stability of the bicycle); see for instance (Escalona and Recuero, 2012). These multi-body models provide realistic dynamics relating the control of the cyclist (e.g. steering angle, pedal force) to the dynamics of the bicycle. Although the model framework presented in this paper is generic regarding the bicycle dynamics model, we have decided to keep this dynamics model as simple as possible, while maintaining the most important features.

In line with the work of Gavriilidou et al. (2017), we use the following model relating the angular acceleration ω_p and the longitudinal acceleration a_p to the direction ϕ_p and longitudinal speed v_p, and the position x_p and y_p:

$$\frac{dx_p}{dt} = v_p \cdot \cos(\phi_p), \qquad \frac{dy_p}{dt} = v_p \cdot \sin(\phi_p) \tag{1}$$

$$\frac{dv_p}{dt} = a_p, \qquad \frac{d\phi_p}{dt} = \omega_p \tag{2}$$

Note that in the remainder, we will drop the subscript p (for individual bicycles) for notational convenience. Also, we will use the state dynamics notation $\frac{d}{dt}\vec{x} = \vec{f}(t, \vec{x}, \vec{u})$ where the state is defined by $\vec{x}_p = (x_p, y_p, v_p, \phi_p)$, and the control $\vec{u}_p = (a_p, \omega_p)$.

Note that the model is not *collision free*. In many pedestrian models, collisions (or rather physical contact) can occur. In many cases, these models have dedicated sub-models that deal with the effect of physical contact (e.g. the social forces model describes impact of normal and friction forces). In this paper, we have refrained from formulating such a submodel and will hence not consider the impact of physical contact or collisions.

Related to this, we also note that we do not explicitly consider the shape of the cyclist. This in part can be included in the physical modelling. At the same time, we can include more advanced mechanical models of the bicycle in the control model used by the cyclist (now reflected by Eqs. (1) and (2)).

4.2. Mathematical framework

In line with the behavioural assumptions discussed in the previous section, we assume that a cyclist will aim to optimise her effort J and choose the corresponding control actions (longitudinal acceleration or braking a, changing direction ω). The effort is determined over a certain oversee-able time span $[t_k, t_k + T)$, and is a function of the control actions during this period as well as the state of the considered cyclist and other cyclists in the nearby environment. Without loss of generality, we use the following specification:

$$J = \int_{t_k}^{t_k+T} e^{-\eta s} L(s, \vec{x}(s), \vec{u}(s)) ds + e^{-\eta(t_k+T)} \Phi(t_k + T, \vec{x}(t_k + T)) \tag{3}$$

where $\vec{x} = (x, y)$ is the state and $\vec{u} = (a, \omega)$ is the control vector. The integrand L describes the so-called running cost (the effort incurred during a short time interval $[s, s + ds)$); Φ denotes the terminal cost, that is, the costs left at the end of the time horizon. Factors that will determine L and Φ are the ability to maintain to a desired speed and direction, cycling too close to other cyclists, spending effort on acceleration and braking, etc.

Let us note that the costs are discounted via the exponential function $e^{-\eta t}$. This function describes the fact that future costs are considered to be less important that present costs. The discount factor $\eta \geq 0$ describes the extent to which this occurs. Discounting is a common way to include the impact of uncertainty about future conditions in the modelling.

The general idea is that the cyclist who we are considering will predict the effort she will incur during $[t_k, t_k + T)$ when applying the control $u_{[t_k, t_k+T)}(\cdot)$ and assuming that the other cyclists will react in a certain way (as explained in Section 4.5). Mathematically:

$$u^*_{[t_k, t_k+T)}(\cdot) = \arg\min J \tag{4}$$

4.3. Cost functions

Let us consider the cost function specification in a bit more detail in this subsection. We will consider three different cost elements: cost of applying a certain control $\vec{u} = (a, \omega)$, cost of straying from the desired speed $v^0 = v^0(t, \vec{x})$ and direction $\phi^0 = \phi^0(t, \vec{x})$, and the cost of being too close to other cyclists.

In doing so, we generally assume that the running cost L is the sum of the attributes L^{accel}, $L^{straying}$, and L^{prox}. In the specifications below, c_a, c_ω, c_v, c_ϕ denote the relative weights of the acceleration and straying cost, compared to the proximity cost.

4.3.1. Control costs

We will use a simple specification of the cost or effort that is incurred by applying a certain control. For the longitudinal acceleration we assume:

$$L_p^{accel,v} = \frac{1}{2c_a} a_p^2 \tag{5}$$

while for the angular acceleration we assume:

$$L_p^{accel,\phi} = \frac{1}{2c_\omega} \omega_p^2 \tag{6}$$

These specifications have been used because they, first of all, satisfy reasonable properties: acceleration incurs cost and deceleration does as well. For the sake of simplicity, we assume these cost to be symmetric (although alternative specifications are easily incorporated). Second of all, the quadratic specification results in the nice property that we can find a closed form expression for the acceleration (both longitudinal and angular) and the so-called co-state or marginal cost, as will be clarified in the remainder.

4.3.2. Straying from the optimal path

We assume that cyclists aim to keep their desired (shortest, most comfortable, safest, etc.) path. We define this path by defining the desired speed path $v^0(t, \vec{x})$ and the desired direction path $\phi^0(t, \vec{x})$, which are both functions of time t and space $\vec{x}$. The latter implies that the path changes in time and over space (in its most generic description).

To keep the model mathematically tractable, we again use simple quadratic expressions. For the desired speed deviations, we propose the following cost specification:

$$L_p^{straying,v^0} = \frac{c_v}{2}(v_p^0 - v_p^2)^2 \tag{7}$$

while for the angular acceleration we assume:

$$L_p^{straying,\phi^0} = \frac{c_\phi}{2}(\phi_p^0 - \phi_p^2)^2 \tag{8}$$

4.3.3. Proximity cost

For the proximity cost, we use the following specification:

$$L_p^{prox} = \sum_{q \in Q} e^{-r_{rp}/R_p^0} \left(\psi_p + (1-\psi_p) \frac{1+\cos\theta_{qp}}{2} \right) \tag{9}$$

with

$$\cos\theta_{qp} = \cos(\phi_p - \beta_{qp}) = \cos(\phi_p) \cdot \cos(\beta_{pq}) + \sin(\phi_p) \cdot \sin(\beta_{pq}) \tag{10}$$

with β_{qp} is the angle of the vector between $\vec{x}_q$ and $\vec{x}_p$, i.e.:

$$\cos(\beta_{pq}) = \frac{x_q - x_p}{r_{pq}} \tag{11}$$

and

$$\sin(\beta_{pq}) = \frac{y_q - y_p}{r_{pq}} \tag{12}$$

with r_{pq} denotes the Euclidean distance between p and q.

Note that via the parameter ψ_p, we can describe the level of anisotropy in the cost. If $\psi_p = 0$, only costs due to cyclists in front are considered (anisotropic cost). For $\psi_p = 1$, the proximity cost are fully symmetric, so cyclists behind are equally important as cyclists in front (isotropic cost).

4.4. Subjective costs minimising conditions and solution approach

We use Pontryagin's minimisation principle to determine the path of the cyclists that minimise their effort. Key to this principle are the so-called co-states, which we will define for each cyclist p. These co-states – of *shadow cost* – describe the marginal cost of the state (i.e. the position in x_p and y_p of the cyclists, the speed or the direction) and are respectively denoted by λ_{x_p}, λ_{y_p}, λ_{v_p}, and λ_{ϕ_p}. The co-states describe the additional cost of changing the state by an infinitesimal value.

The dynamics of the co-states can be determined using the so-called Hamiltonian:

$$H = L + \vec{\lambda} \cdot \vec{f} \tag{13}$$

which is an auxiliary function used to determine the necessary condition for optimality. One of these conditions is the so-called *stationarity condition*, which states that for the optimal control, we have:

$$H(t, \vec{x}^*, \vec{u}^*, \vec{\lambda}^*) \leq H(t, \vec{x}^*, \vec{u}, \vec{\lambda}^*) \tag{14}$$

for all admissible controls $\vec{u}$. Using the specifications of the cost that were presented earlier in the paper, we get:

$$a^* = -c_a \cdot \lambda_v \tag{15}$$

and

$$\omega^* = -c_\omega \cdot \lambda_\phi \tag{16}$$

These expressions show that the optimal longitudinal and angular accelerations are determined from the co-states (or marginal cost) of respectively the speed v and the direction ϕ. This means that if e.g. the marginal cost of the speed is positive, the acceleration is negative (to locally reduce the speed and thus the cost).

The co-state dynamics are given by the following set of equations:

$$-\frac{d}{dt}\vec{\lambda} = \frac{\partial}{\partial \vec{\lambda}} H \tag{17}$$

with terminal conditions $\vec{\lambda}(t+T) = \frac{\partial}{\partial \vec{\lambda}} \Phi(t+T, \vec{x}(t+T))$ determined from the terminal costs.

Combined with the state dynamics described by Eqs. (1)–(2) and initial state conditions $\vec{x}(t) = \vec{x}_t$, we have a fully determined system. As is explained in Hoogendoorn et al. (2012), the resulting problem is a mixed initial–terminal value problem, which is not trivial to solve. We use the iterative method outlined in Hoogendoorn et al. (2012) to numerically approximate the optimal solution.

Note that the approach is flexible and can be applied to essentially any effort function specification and state dynamics (including e.g. vessel dynamics (Hoogendoorn et al., 2013)).

4.5. Interaction strategies

Next to using a dynamics model that mimics the dynamics of a bicycle (including cyclist), one of the major contributions of our approach is the ability to model different strategies that a cyclist can adopt. Similar to Hoogendoorn et al. (2013), we consider the following strategies:

- *Cooperative opponents cyclist.* In this situation, the considered cyclist assumes that the cyclist she is aiming to avoid will *cooperate* in the evasive manoeuvre. The cyclist is thus – in a sense – risk prone, since she relies on the cooperative behaviour of the opponent cyclist.
- *Zero-acceleration behaviour of opponent bicycles.* This is the most simple situation where the cyclist assumes that the cyclist she is aiming to avoid will maintain her current direction and speed. The cyclist is *risk neutral*.
- *Demon opponent cyclists.* This situation describes the case where the cyclist is risk averse, considering the worst-case scenario when the cyclist she is trying to avoid is actively aiming to hit her. This could be the case when the other cyclist is not paying any attention to her surrounding.

We will model the different interaction strategies using different specifications of the cost function for the considered cyclist p and her opponents q. In the *cooperative case*, p assumes that the cost function of q is the same as her own. This implies that the opponents aim to move away from the considered cyclist in the same way as she is trying to move away from the opponent. In other words, both p and q consider — in the mental model of p the same proximity cost (Eq. (9)).

For the *demon opponent model*, cyclist p assumes that her opponents aim to come as close as possible. This means that while p considers proximity cost Eq. (9), she assumes that the opponents have a negative proximity cost, i.e. $\tilde{L}_q^{prox} = -\zeta \cdot L_q^{prox}$ for $\zeta > 0$.

In the *zero acceleration model*, p assumes that opponents q will not try to move away or move towards p. This is again modelled via the proximity cost model used for the demon opponent model, but with $\zeta = 0$ (i.e. q does not consider proximity cost).

Let us note that in our experiments described in Yuan et al. (2018) and Gavriilidou et al. (2019b), different strategies have been observed in different scenarios considered (e.g. head-on interaction, merging and crossing scenario). For the crossing scenarios, this is revealed by differences in gap acceptance behaviour, the extent to which right-of-way rules are adhered to, differences in distance keeping, etc. Our main aim is to see how we can conceptually model such differences, without presenting a calibrated model per se.

As a final remark, it should be clear that the strategies – and thus the parameter associated with it – are *latent* and cannot be observed directly. In observing the parameter, we need to rely on observable behaviour as manifested in microscopic flow characteristics, e.g. the trajectories (e.g. those observed in the controlled experiments described in Yuan et al. (2018) and Gavriilidou et al. (2019b)). Given that the outcomes of the simulations are sensitive to the assumed strategies, indirect determination of the parameter seems possible. We do presume however that microscopic data are needed, given the large differences in behaviour (and thus strategies) observed.

4.6. Traffic rules

Contrary to pedestrian behaviour, in which few – often unwritten – rules dictate walking behaviour, cyclists are more included to adhere to regulations, albeit often not in the same extent as car traffic. For the European situations this for instance means that cyclists from the right have right-of-way, and that overtaking occurs on the left hand side.

There are different ways to add these traffic rules to the modelling framework. Depending on the strictness of the rules, we could opt for changing the specification of the cost functions (in case of softer adherence to regulations). For instance, we could change the proximity cost in Eq. (9) by adding an off-set to the angle between the direction ϕ_p and the angle between the position of p and of the opponent q, i.e.

$$\tilde{\theta}_{pq} = \theta_{pq} + d\theta^0 \tag{18}$$

This off-set will cause a natural preference to overtake on the left ($d\theta^0 > 0$) or on the right ($d\theta^0 < 0$). Note that this does require a distinction based on whether the opponent is overtaking or is coming from the opposite direction.

Rules that are adhered to more strictly could be modelled in a different way, e.g. via the interaction strategies: the cyclist that has to yield will adhere to the cooperative opponent strategy or to the demon opponent strategy, while the cyclist having right-of-way would adhere to the zero-acceleration strategy. Another approach is that the cyclists having right-of-way simply ignore the effort due to those cyclist that have to yield, i.e.:

$$L_p^{prox} = \sum_{q \in \tilde{Q}} e^{-r_{rp}/R_p^0} \left(\psi_p + (1 - \psi_p) \frac{1 + \cos\theta_{qp}}{2} \right) \tag{19}$$

where $\tilde{Q}$ is the set of opponents to whom p reacts (i.e. excluding those cyclists that have to provide priority).

In the remainder of the paper, we will look at different scenarios to show the (qualitative) behaviour of the model. We will look at the impact of different model parameters and strategies, in particular focusing on impacts of collective phenomena (e.g. self-organisation). Section 5 first discusses the behaviour in case of one-on-one interactions. Section 6 shows impacts of parameters on collective behaviour. Each section starts with a short description of the experimental set-up, including the research questions we aim to answer. Where relevant and possible, we compare the outcomes of the simulation with the experimental outcomes of Yuan et al. (2018) and Gavriilidou et al. (2019b).

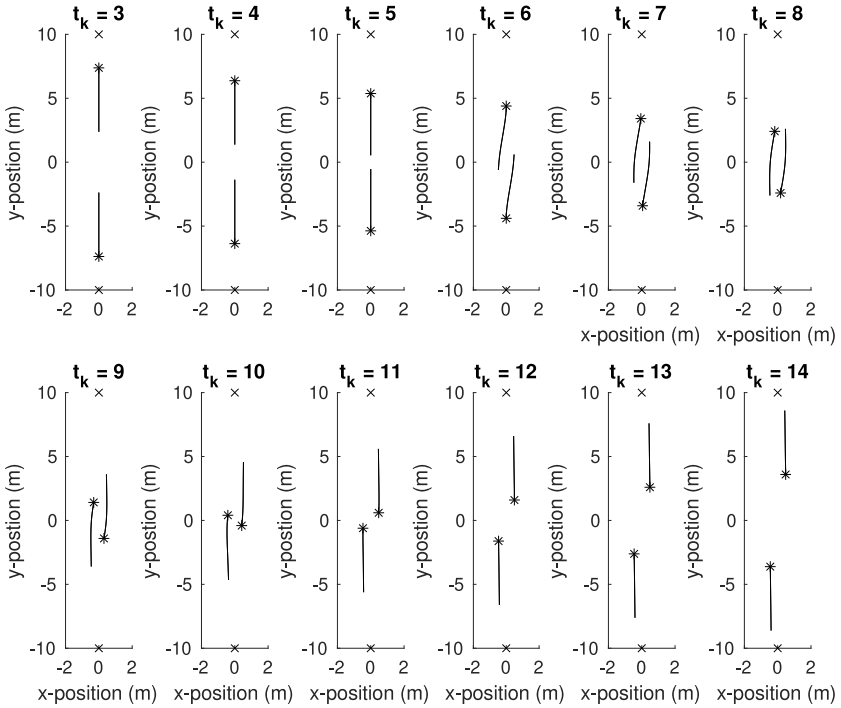

Fig. 2. Example of model behaviour for head-on interaction between two cyclists for $T = 5$ s.

5. Model behaviour for one-on-one interactions

In this section, we show examples illustrating the behaviour of the model. We consider three scenarios (head-on interactions, overtaking, and crossing). We show the impact of the *parameter choice* on the behaviour of the models, in particular on the efficiency and safety of the interaction. We will also show the impact of the interaction strategy. Our aim is to show the model's plausible behaviour, and the impact of the parameter choices thereon.

We will use the concept of efficiency based on the ideas proposed by Helbing and Verkehrsdynamik (1996). The term is defined as follows:

$$E = \int_{t_0}^{T} \frac{1}{N} \sum_{p=1}^{N} \frac{\vec{v}_p(t) \cdot \vec{e}_p^0(t)}{v_p^0(t)} dt \tag{20}$$

where $\vec{v}_p(t)$ is the current velocity, $\vec{e}_p^0(t)$ denotes the current optimal direction, and $\vec{v}_p^0(t)$ denotes the optimal current velocity of bicycle p a time instant t. For the experiments considered in this section, the efficiency concept is equivalent to the realised average speeds in the planned direction of the cyclists. For 'safety', we will use the minimum distance between the interacting cyclists.

5.1. Head-on interactions

Fig. 2 shows the results for a head-on interaction, where cyclists have a preference to pass on the right in case of a head-on interaction. In the figure (and all figures presented in the remainder), the star '*' shows the current position of the cyclists at time instant $t_k = 3\text{ s}, 4\text{ s}, 5\text{ s}, \ldots$. The lines show the path the cyclist predicts – and attempts to execute – in the interval $[t_k, t_k + T)$, where T denotes the prediction horizon. The cost components in the example are the cost of acceleration and deceleration, the cost of straying from the desired path towards the destination, and the cost of cycling too close to other cyclist, as specified in Section 4. We assume full anisotropy ($\psi = 0$) for this particular case, as well as the cooperative strategy.

The model behaves in a plausible manner: when the longitudinal distance between the cyclists becomes sufficiently small (from $t_k = 6$ s onward), both cyclists start to make a manoeuvre to evade the approaching cyclist. Note that both cyclists make an evasive manoeuvre to the right and that due to the cooperative strategy considered here, they will anticipate on the planned reaction of the opponent cyclist.

5.1.1. Parameter impact

Different parameters of the model influence the interaction characteristics. In particular, we see that the prediction horizon T has a strong impact on the encroachment distances that cyclists reveal upon interaction (the smaller T, the later evasive manoeuvres are

Table 1
Impact of prediction horizon on speed and distance.

T (in s)	$E(v_1)$	$E(v_2)$	min(d)
1.0	0.9010	0.8937	0.5387
2.5	0.9106	0.9096	0.8137
5.0	0.9156	0.9156	1.0760
10.0	0.9153	0.9152	1.1638
$c_\phi^0 = 0.1$	0.9129	0.9129	1.3858
$c_\phi^0 = 5$	0.9109	0.9109	0.7533
$c_v^0 = 0.1$	0.7937	0.7937	1.1246

started and the closer the cyclists approach each other). In Table 1 we provide an overview of the impact of the prediction horizon T on the average speed of the two cyclists and the minimum distance between them (please note that all numbers are normalised). We see that the prediction horizon causes a (slight) increase in the average speed, while the minimum distance increases substantially. In other words, higher anticipation levels have a limited (positive) impact on efficiency, but do cause a substantially safer interaction.

We also considered the impact of the cost of straying from the desired direction or speed by changing the weights c_ϕ^0 and c_v^0 respectively (see Table 1). Similar to the results we will present for the other scenarios, lower values of c_ϕ^0 (lower costs due to angular straying from the optimal path) lead to more agile behaviour of the cyclists. This leads to larger distances between the interacting cyclists (proximity cost have a higher relative weight in the total cost than keeping the desired direction). For higher values of c_ϕ^0, the opposite occurs, meaning that cyclists stick more to their desired direction. Smaller values of c_v^0 lead to relatively larger reductions in the speed, since cyclists have more limited inclination to maintain their desired speed.

5.1.2. Impact of strategy

The previous experiments considered the situation where the considered cyclist p assumes that the opponent follows the same strategy as she does. That means that the opponent effectively cooperates. Fig. 3 shows the results for the head-on interaction case if we consider the demon opponent strategy with $\zeta = 0.8$, assuming that both cyclists use this strategy. From the figure, we see that both cyclists make a large circumventing movement to ensure that the opponent will not be able to cause a crash. This is in particular visible for $t_k = 6$ s, where the predicted movement of both cyclist shows a large evasive manoeuvre. For the instants $t_k = 7$ s, 8 s, …, this evasive manoeuvre is smaller because the opponent has fewer possibilities to reach her. In the end, the lateral distance of passing is far larger (more than 1) compared to the cooperative case (around 0.7). For the zero acceleration case, we see that the result holds the middle ground between the other scenarios (no figure).

As a final note, we have compared the outcomes of the simulations with the experiments described in Yuan et al. (2018). In these experiments, each rider passes on the left hand side (which is in line with Dutch traffic regulations). The microscopic data collected shows that the minimum passing distance is about 1 metre, occurring at the time the riders pass each other. At that time, a lateral swerving movement is observed, as can be seen from our simulations as well. In general, after the interaction, the riders return to their original lateral position.

5.2. Overtaking interactions

Fig. 4 shows an example of the model behaviour in case of an overtaking. We will use this scenario as a base case. We assume full anisotropy ($\psi = 0$), and $d\theta^0 = 0.1$. Again, we see that the model behaves in a plausible way: the faster cyclist (cycling 25% faster than the slower one) $p = 1$ stays behind the slower cyclist $p = 2$ for some time and then performs an overtaking manoeuvre. Since this scenario assumes full anisotropy, the overtaken cyclist does not respond while being overtaken.

5.2.1. Parameter impact

Table 2 shows some of the characteristics of the simulation results for different scenarios, including different prediction horizons T, isotropic interactions ($\psi = 1$), and other values of θ^0.

Regarding the prediction horizon, we see a similar outcome as in the case of the head-on interaction: a larger prediction horizon (more anticipation) results in higher efficiency (in this case mostly for the overtaker) and safer interactions (large encroachment distances). Also for the values of c_ϕ^0 and c_v^0, we find similar results as in the head-on interaction case.

Anisotropy results in (mainly) one-sided interactions in case of an overtaking. In case of isotropic interactions, we see that the cyclist being overtaken is influenced (average speed is higher than in the other cases, in fact it is higher than the desired normalised speed of 1). In other words, the overtaken cyclist speeds up.

Finally, in case $d\theta^0 = 0$, we see that the overtaker will actually not overtake at all (since it cannot decide to overtake on the left or the right), and keeps following the slow cyclist in front.

Without going into detail, comparing the outcomes of this simulation to the results of our controlled experiment where overtakings where observed (see Gavriilidou et al. (2019b)), we see a large variation of context dependent manoeuvres. For the crossing flow experiment, we see many – but not only – left-hand-side overtakings, most of which are anisotropic on nature (although occasionally we see the overtaken rider swerve a bit to the right). For the bottleneck experiment, we see that fewer overtakings take place while cyclists are anticipating on the narrowing of the road, showing the impact of the prediction horizon.

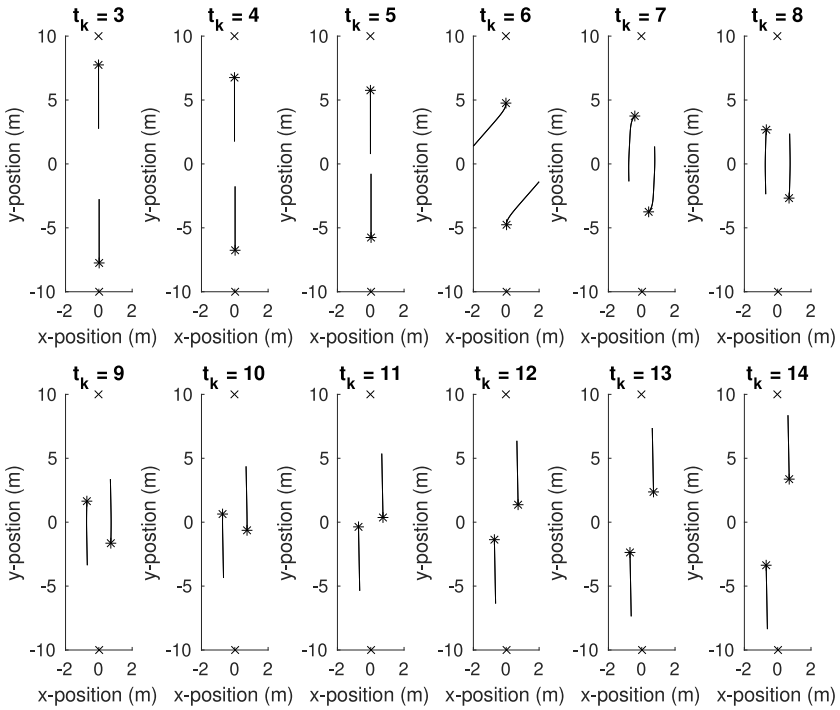

Fig. 3. Example of model behaviour for head-on interaction between two cyclists for $T = 5$ s assuming the *demon opponent interaction strategy*.

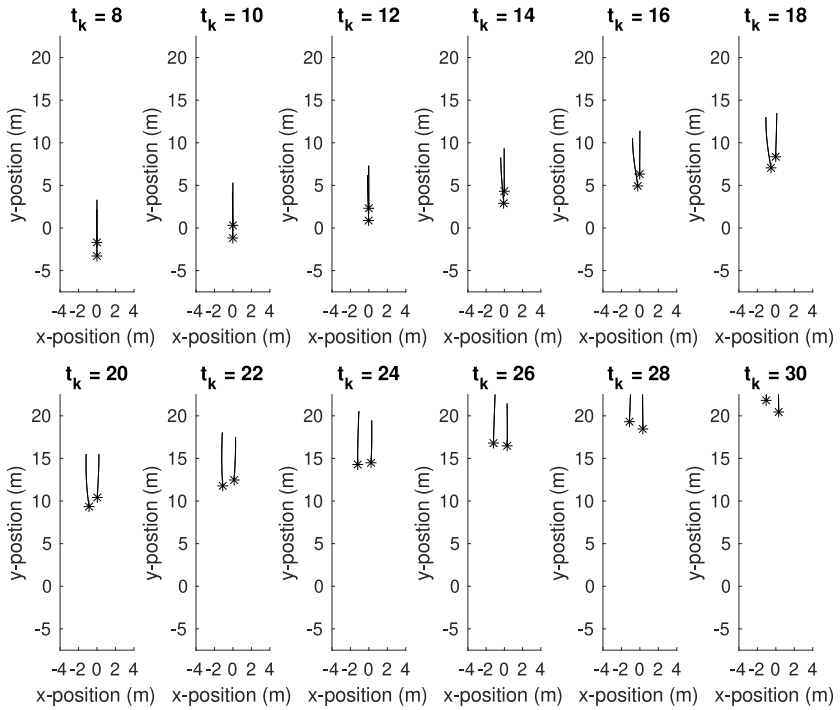

Fig. 4. Example of model behaviour for overtaking for $T = 5$ s.

Table 2
Impact of prediction horizon on speed and distance.

Scenario	$E(v_1)$	$E(v_2)$	min(d) (in m)
Base case	1.1210	0.9647	1.4255
$T = 1.0$	1.0911	0.9529	0.7982
$T = 2.5$	1.0962	0.9646	1.1780
$T = 10.0$	1.1759	0.9630	1.540
$c_\phi^0 = 0.1$	1.1653	0.9357	1.7036
$c_\phi^0 = 5$	0.9977	0.9353	1.4093
$c_v^0 = 0.1$	0.9367	0.8915	1.7360
$\psi = 1$	1.1029	1.0560	1.5942
$d\theta^0 = 0$	1.0117	0.9606	1.4556

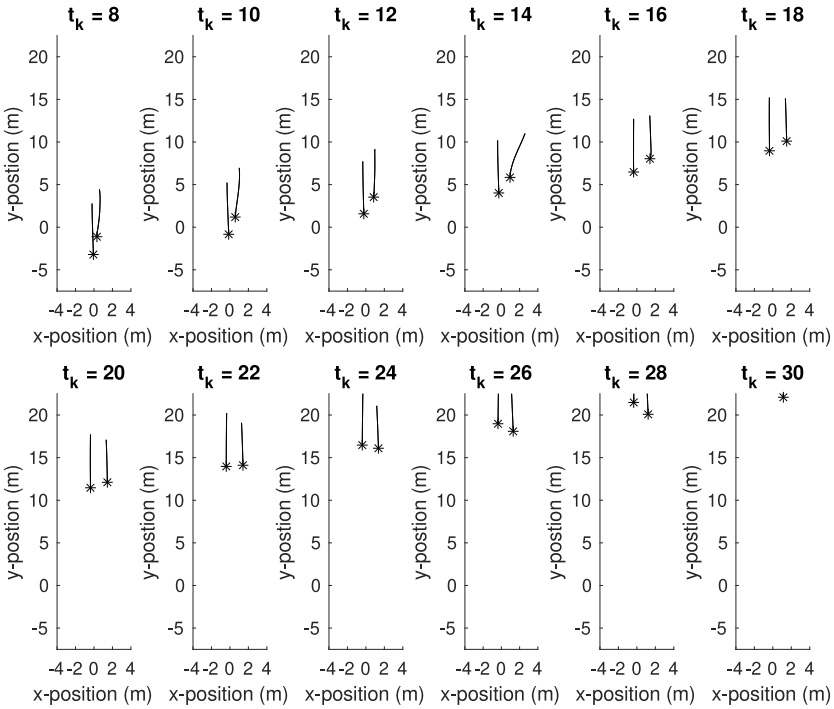

Fig. 5. Example of model behaviour for overtaking between two cyclists for $T = 5$ s assuming the *demon opponent interaction strategy*.

5.2.2. Impact of strategy

The previous experiments consider the situation where the considered cyclist p follows a cooperative strategy, and assumes that the opponent follows the same strategy. Fig. 5 shows the results for the overtaking interaction case if we consider the demon opponent strategy with $\zeta = 0.8$, assuming that both cyclists use this strategy. The figure shows that in this case, both cyclists will make an evasive manoeuvre, even though we consider an anisotropic proximity cost function. This is because the slow cyclist $p = 1$ assumes that the opponent cyclist will attempt to come as close as possible, also resulting in a cost for $p = 1$. Again, the zero-acceleration case shows similar results, albeit less pronounced.

5.3. Crossing interactions

Fig. 6 shows the results for a crossing interaction, assuming again full anisotropy ($\psi = 0$) and a cooperative strategy for both cyclists in this case. The model behaves in a plausible manner: when the distance between the cyclist becomes sufficiently small (from $t_k = 6$ s onward), cyclists start to make a manoeuvre to evade the approaching cyclist. Note that both cyclists will make an evasive manoeuvre and that due to the cooperative strategy considered here, they will anticipate on the planned reaction of the opponent cyclist.

In this case, we see that the cyclist coming from the right gets priority and passes in front of the cyclist coming from the left. This is coincidental and caused by small numerical approximation differences in the solution scheme. We do note that by defining $d\theta^0$, we can control a (soft) preference for passing in front or in the back.

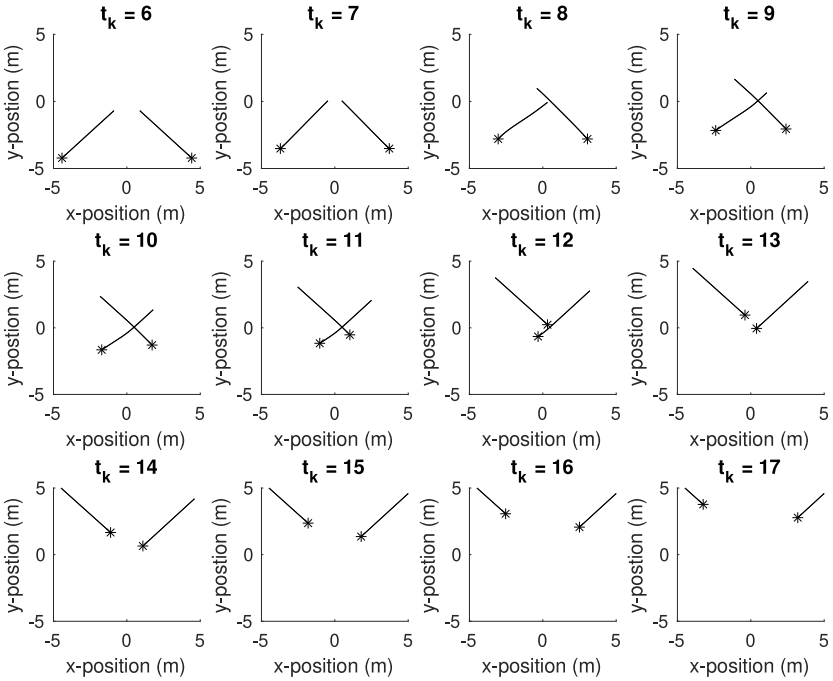

Fig. 6. Example of model behaviour for crossing interaction between two cyclists for $T = 5$ s.

Table 3
Impact of prediction horizon on speed and distance.

T (in s)	$E(v_1)$	$E(v_2)$	min(d) (in m)
1.0	0.8961	0.9099	0.7821
2.5	0.8957	0.9330	0.9500
5.0	0.8946	0.9323	1.0492
10.0	0.8881	0.9337	1.1971
$c_\phi^0 = 0.1$	0.9284	0.9190	1.3136
$c_\phi^0 = 5$	0.8719	0.9358	1.0780
$c_v^0 = 0.1$	0.8619	0.7471	1.2544
$\zeta = 0.8$	0.9407	0.9121	1.4392
$\zeta = 0$	0.8967	0.9412	1.2169

5.3.1. Parameter impact

In Table 3 we provide an overview of the impact of the prediction horizon T on the average speed of the two cyclists and the minimum distance between them. We see that the prediction horizon causes a (slight) increase in the average speed, while the minimum distance increases substantially. In other words, higher anticipation levels have a limited (positive) impact on efficiency, but do cause a substantially safer interaction.

In particular in this type of interaction, it is of interest to see what happens if other parameters change. Table 3 shows the impact of changing the weights of longitudinal acceleration c_v^0 and angular acceleration c_ϕ^0. For instance, Fig. 7 shows the results for the crossing interaction in case of a low weight for the angular acceleration ($c_\phi^0 = 0.1$). This reduction of the cost of angular acceleration causes the behaviour of the cyclist to be more volatile: changes in longitudinal speeds are relatively expensive, so the cyclists will change their direction more easily. From the table, we observe that different values yield different results in terms of speed and distances.

5.3.2. Impact of strategy

The previous experiments consider the situation where the considered cyclist p assumes that the opponent follows the same strategy as she does. That means that the opponent effectively cooperates. Fig. 8 shows the results for the head-on interaction case if we consider the demon opponent strategy with $\zeta = 0.8$, assuming that both cyclists use this strategy. From the figure, we see that both cyclists make a larger circumventing movement to ensure that the opponent will not be able to cause a crash. In the end, the minimum distance is much larger than in case of the cooperative interaction (1.4 m compared to 1.0 m). For the zero-acceleration opponent, the minimum distance value lies in between (1.2 m).

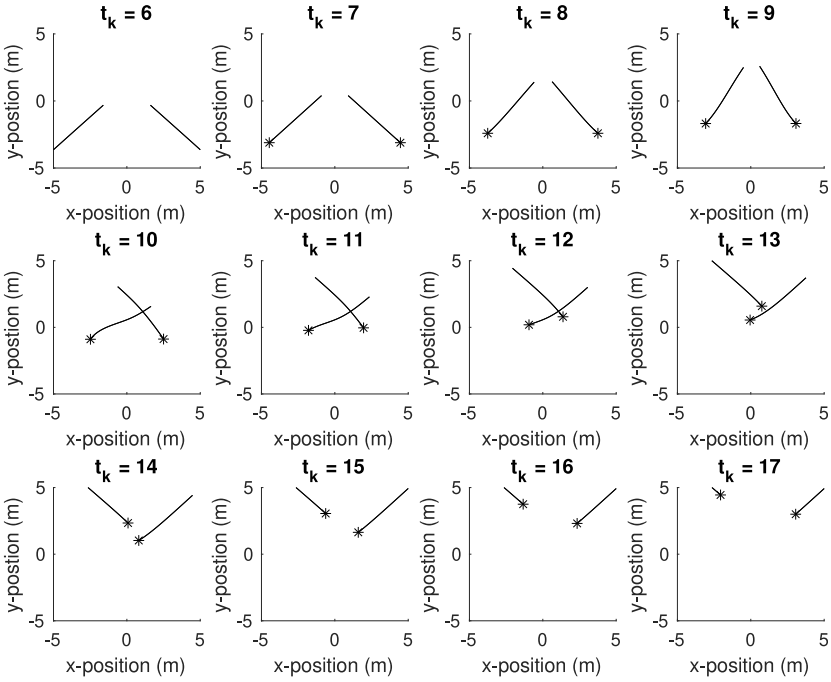

Fig. 7. Example of model behaviour for crossing interaction between two cyclists for $T = 5$ s and $c_{\phi}^{0} = 0.1$.

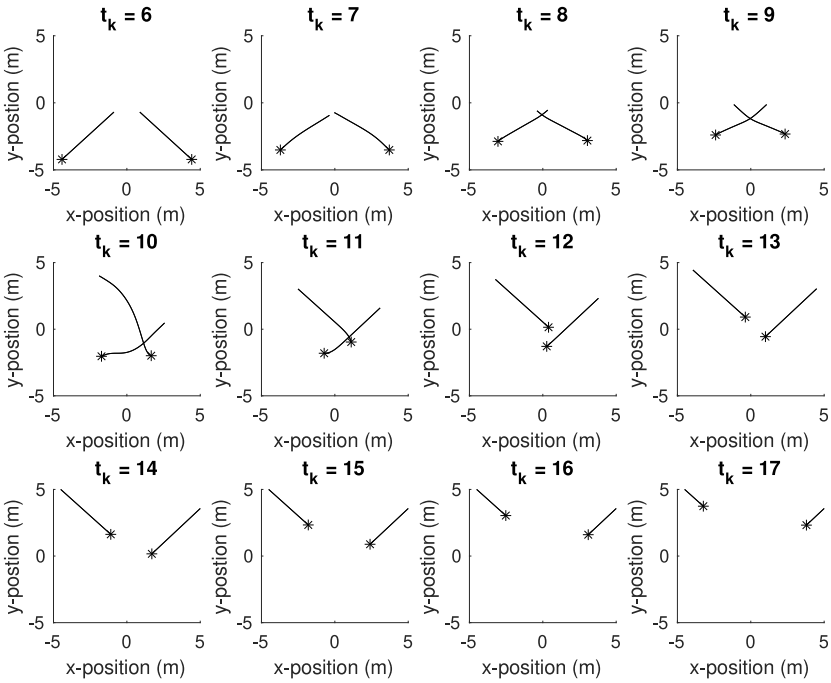

Fig. 8. Example of model behaviour for head-on interaction between two cyclists for $T = 5$ s assuming the *demon opponent interaction strategy*.

Comparing the outcomes of the simulations with the experiments from Gavriilidou et al. (2019b), we can conclude that qualitatively, the different outcomes we observe are also observed in the experiment. There is substantial heterogeneity in observed behaviour, which can be explained by differences in prediction horizon between cyclists, as well as different risk attitudes.

Table 4
Impact of prediction horizon on speed and distance.

Scenario	min. eff.	mean eff.	max eff. σ	mean eff. σ
Base case	0.7935	0.8904	0.1698	0.1006
$T = 1.0$	0.9340	0.9843	0.0746	0.0345
$T = 2.5$	0.9432	0.9829	0.0496	0.0209
$T = 10.0$	0.7507	0.8776	0.3115	0.1921
$\psi = 1$ and $T = 1.0$	0.9644	0.9963	0.1824	0.0539
$\psi = 1$ and $T = 2.5$	0.9452	0.9887	0.0727	0.0318
$\psi = 1$ and $T = 5.0$	0.8292	0.9632	0.1701	0.0843
$c_\phi^0 = 0.1$ and $T = 2.5$	0.9603	0.9818	0.0376	0.0162
$c_\phi^0 = 10$ and $T = 2.5$	0.0608	0.4693	0.3258	0.1016
$c_v^0 = 10$ and $T = 2.5$	0.9857	0.9947	0.0192	0.0074

6. Self-organisation and the conditions under which it occurs

Little is known about self-organisation in relation to bicycle flows. To a large extent, this is due to the fact that few data are available for interaction scenarios which potentially result in self-organisation. Some evidence, however, exists of forms of self-organisation. For instance, in the experiments described in Gavriilidou et al. (2019b), the so-called 'zipper effect' was observed in the bottleneck scenarios. At the same time, spontaneous formation of jam waves were identified in experiments done by Guo et al. (2019).

In this section, we will show how the model performs in situations with multiple cyclists. We will in particular investigate the extent in which self-organisation occurs in relation to model parameters (e.g. prediction horizon, heterogeneity). It is interesting to see that unlike pedestrian flows, in which self-organisation is very common, the very nature of the cyclist dynamics result in far stricter self-organisation conditions (e.g. less heterogeneity, specific parameter ranges in which self-organisation occurs, etc.). We will assess the level of self-organisation visually as well as via the *efficiency indicator* introduced by Helbing (Helbing and Verkehrsdynamik, 1996); see Eq. (20).

Note that next to more dynamic features, such as self-organisation, other collective flow characteristics can be established from the model. This can be done by means of simulation (e.g. for a bottleneck situation), or via mathematical analyses (e.g. assuming zero acceleration cases) of the equilibrium conditions. Such analyses are relatively straightforward and provide interesting insights in how model parameters relate to equilibrium conditions (e.g. the fundamental diagram); see Hoogendoorn and Bovy (2003).

6.1. Head-on interactions

The first example consists of two groups of cyclists that are moving in opposite directions. We assume a slight preference for moving to the right upon having an head-on interaction ($\theta^0 = -0.01$). In Table 4, we provide an overview of some of the resulting characteristics of the simulation, where the base case refers to the situation with a prediction horizon $T = 5$ with full anisotropy $\psi = 0$.

The table shows how the efficiency depends on some of the model parameters. In particular, we see that the prediction horizon has an interesting impact. For large values of the horizon ($T \geq 5$), we see that the efficiency is generally lower than in case of lower prediction horizons. For the scenarios considered, the most efficient case (with also the smallest variance in efficiency over the participants and over time) is when we have a prediction horizon of 2.5 s. Apparently, for the collective operations to be most efficient, the prediction horizon should not be too small or too large.

The key to explaining this finding is in the extent to which self-organisation occurs. Fig. 9 shows the results for $T = 2.5$ s. Here, we see forms of self-organisation which are comparable to bi-directional lane formation in pedestrian flows. For this example, six lanes are formed in total. For larger prediction horizons ($T \geq 5$ s), we observe that lanes are less stable or not formed at all.

Another interesting finding is the impact of anisotropy. The isotropic model ($\psi = 1$) shows reduced efficiency compared to the anisotropic case ($\psi = 0$). This outcome is not trivial, since in the isotropic case, cyclists are pushed from behind and are generally expected to show higher average speeds. However, the pushing results in reduced self-organisation.

Next to the anisotropy, we have looked at the impact of sticking to the desired speed or direction. We have done this by testing different values of the cost weights c_v^0 and c_ϕ^0. In illustration, Fig. 10 shows the result for the case where $c_\phi^0 = 0.1$, implying a far smaller contribution of moving from the desired direction than in the base case which had $c_\phi^0 = 1$. In this case, self-organisation still occurs. In fact, the flow becomes slightly more efficient in this case (see Table 4). For the case $c_\phi^0 = 10$, no self-organisation occurs. In fact, the cost of moving away from the desired direction becomes so large that all cyclists stick to the desired value. Upon approaching each other, all cyclists come to a complete standstill eventually. Increasing the cost of the desired speed has a similar impact, but in this case the cyclists try harder to maintain the desired speed. Self-organisation still occurs, and the flow is efficient, as can be seen from Table 4.

Let us note that in Gavriilidou et al. (2019b), no head-on interaction scenarios have been considered. We do however see self-organisation occurring when slow and fast cyclist meet: the fast stream separates from the slow moving riders.

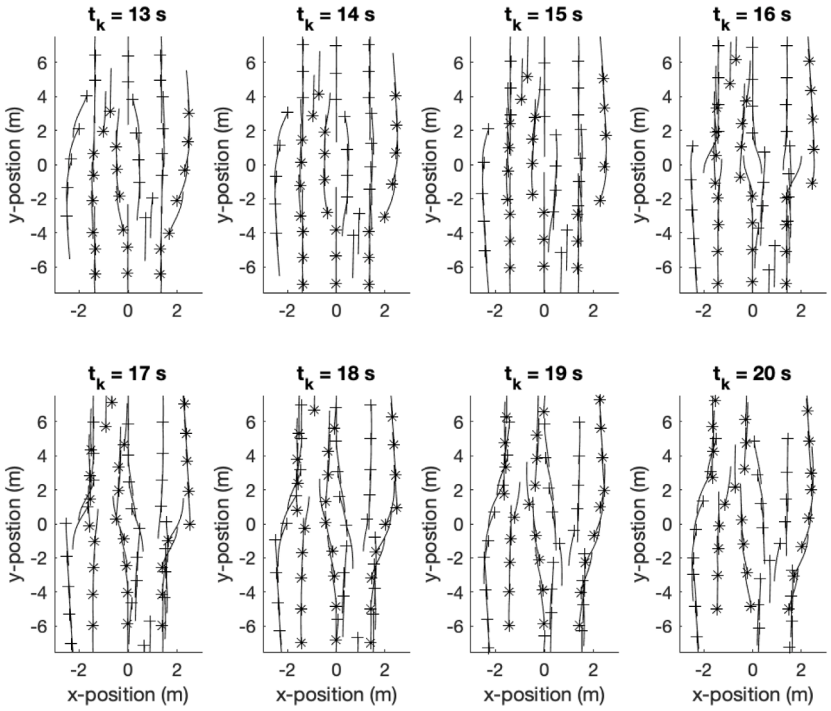

Fig. 9. Example of model behaviour for head-on interaction between multiple cyclists for $T = 2.5$ s.

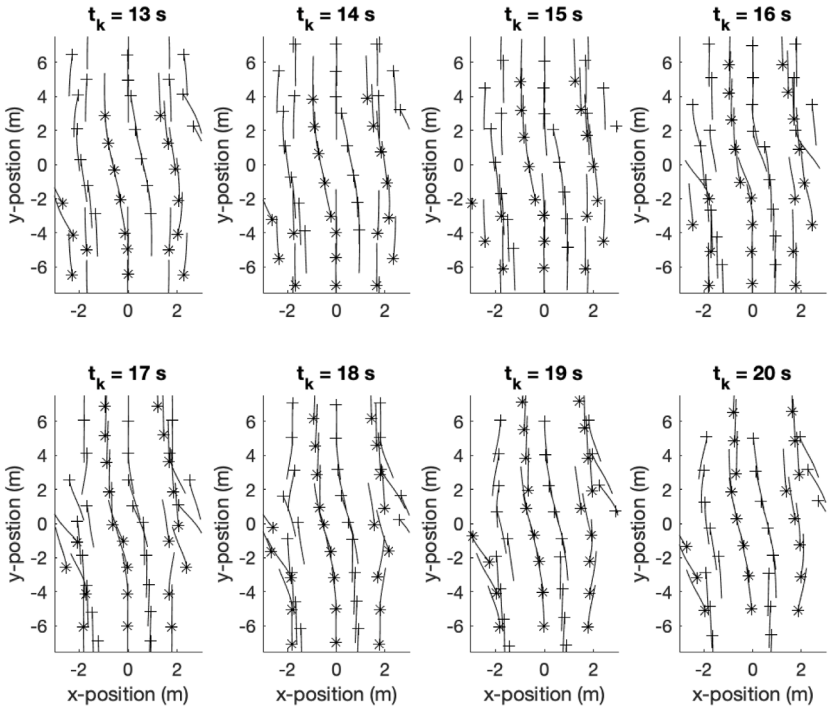

Fig. 10. Example of model behaviour for head-on interaction between multiple cyclists for $T = 2.5$ s. The left figure shows the trajectories; the right figure shows the speeds of the cyclists are a function of time.

Table 5
Impact of prediction horizon on speed and distance.

Scenario	min. eff.	mean eff.	max eff. σ	mean eff. σ
Base case	0.6943	0.8838	0.4282	0.1550
$T = 1.0$	0.8751	0.9526	0.1703	0.0597
$T = 2.5$	0.7743	0.9174	0.2411	0.0880
$T = 10.0$	0.2824	0.5091	0.7267	0.4919
$\psi = 1$ and $T = 1.0$	0.9673	0.9923	0.1736	0.0583
$\psi = 1$ and $T = 2.5$	0.9535	0.9912	0.1607	0.0529
$\psi = 1$ and $T = 5.0$	0.6811	0.8997	0.4755	0.1835
$c_\phi^0 = 0.1$ and $T = 2.5$	0.8027	0.9403	0.1588	0.0694
$c_\phi^0 = 10$ and $T = 2.5$	0.8639	0.9706	0.2424	0.1112
$c_v^0 = 10$ and $T = 2.5$	0.9601	0.9930	0.0686	0.0145

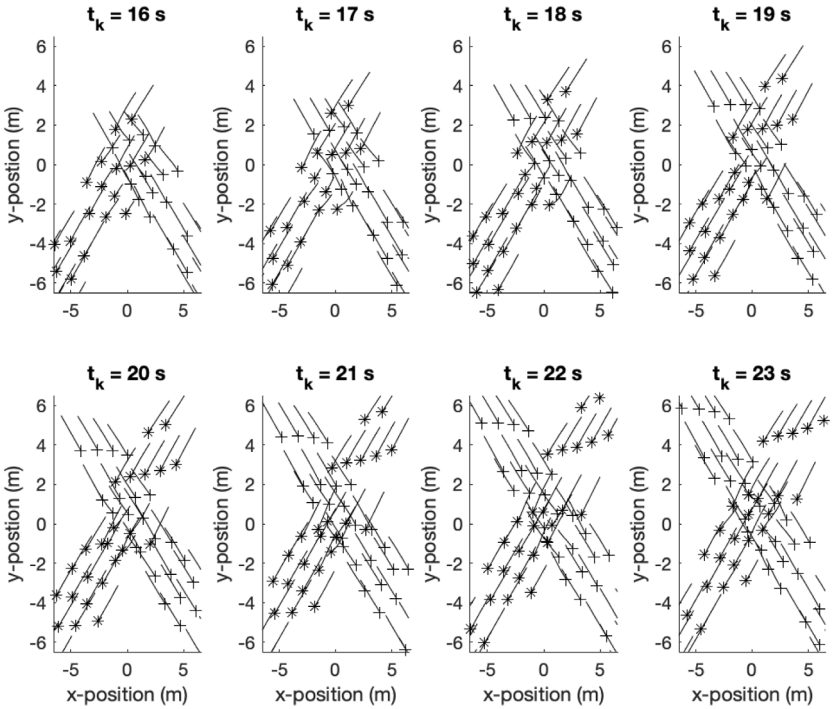

Fig. 11. Example of model behaviour for crossing flow for multiple cyclists for $T = 2.5$ s.

6.2. Crossing flows

As a final example, we have considered crossing flows. Table 5 shows the flow efficiencies for different values of the prediction horizon T and for both anisotropic and isotropic flows. The results are quite similar to the head-on interaction case regarding the impact of the prediction horizon.

Contrary to the head-on interaction case, we see that the isotropic flow performs better – as initially expected – than the anisotropic flow.

Fig. 11 shows the behaviour in case of a crossing flow for a number of one-second consecutive time steps. The figure shows a form of self-organisation. Looking at $t_k = 18$ s as an example, we see the formation of diagonal stripes, also observed in pedestrian flow. This results in a flow which is quite efficient, as was observed in Table 5. This type of self-organisation does not occur for larger prediction horizons (e.g. $T \geq 5$ s), while it does occur for smaller prediction horizon values (see Fig. 12).

From Table 5 we observe that the isotropic model has similar self-organisation properties. Judging from the efficiency variation statistics, the impact of (an-)isotropy is quite limited.

Finally, we have considered the impact of c_v^0 and c_ϕ^0, the parameters that describe the cost if maintaining the desired speed or direction. In illustration, Fig. 13 shows a series of consecutive snapshots for the case that c_ϕ^0 is 0.1 (instead of the original 1). Reducing the c_v^0 results in the desired direction being less adhered to, which can be clearly observed from the figure. The overall efficiency is slightly increased, which could be caused by the fact that the increased manoeuvrability has a positive impact on the efficiency. On the contrary, in case $c_\phi^0 = 10$, we see a substantial reduction of the efficiency.

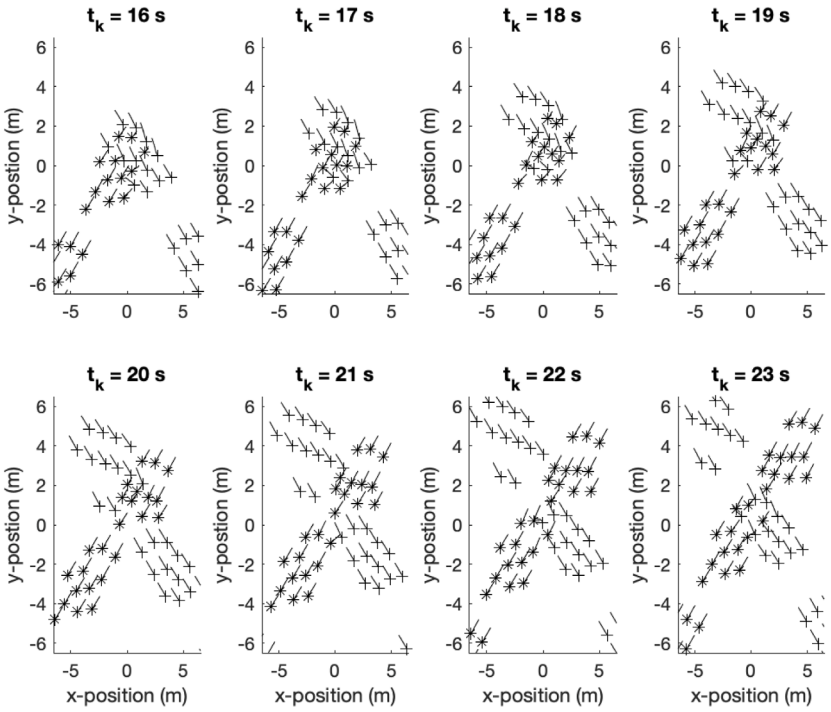

Fig. 12. Example of model behaviour for crossing flow for multiple cyclists for $T = 1.0$ s.

As a final note, the crossing flow experiment of Gavriilidou et al. (2019b) shows occasional self-organisation in particular when groups of risk-neutral or risk-prone cyclists interact. In these cases, the diagonal patterns observed in our simulation can be recognised. However, due to the large variety in cyclist behaviour, these patterns are short lived.

7. Conclusions and future work

This paper derives a game-theoretical model for the operational behaviour of cyclists, by generalisation of our previous work on pedestrian flow.

The main contributions of the paper are first of all in the generalisation itself and second of all in the insights gained by simulation with the model by considering different scenarios, different parameter values, and different interaction strategies.

As the paper explains, the generalisation entails two major changes compared to our previous models. First of all, the model does justice to the kinematics of cyclists. On the contrary to pedestrians, cyclist are more restricted in their movement. The model approximates these restrictions by considering speed and direction and changes therein rather than velocity and (Cartesian) accelerations. The framework is generic in the sense that more involved kinematic models can be included easily. Also, we show how the model can be generalised further by including traffic rules.

Secondly, the model includes different strategies (cooperative, zero-acceleration, demon opponent) in its underlying game-theoretical framework. This allows us to model different attitudes towards risk, for instance when overtaking or meeting another cyclist head-on. We see that the model behaves differently and plausibly in case we consider different strategies.

The (qualitative) insights gained by application of the model pertain to one-on-one interactions and the impact of the strategy assumptions and parameter choices, as well as on the collective phenomena that occur and their sensitivity to parameters (reflecting the extent of the prediction horizon, the level of anisotropy, and the relative importance of sticking to the desired path). We look at efficiency and at self-organised patterns.

First of all, we conclude that the model shows self-organised patterns, with the right choice of model parameters. This is not trivial, given the kinematic model used. This means that it is possible that bicycle flows also reveal self-organised patterns in reality.

We see that the prediction horizon has a large effect on these self-organised patterns. Paradoxically, the longer the prediction horizon, the smaller the probability that self-organisation occurs. When cyclists interacting within a group and with other groups of cyclists look ahead (for more than 2.5 s), optimisation results in complex paths that optimises the individuals objectives. Yet, the complex paths yield poor system performance. Isotropic flows are not more efficient than anisotropic flows. The flow efficiency is also sensitive to the extent to which cyclists adhere to their desired speed and direction.

We conclude that the model acts in a plausible manner, also if we qualitatively compare the model to the experimental data from Yuan et al. (2018) and Gavriilidou et al. (2019b). While we do not aim to show absolute validity, we see that the qualitative behaviour of one-on-one interactions is plausible. We also observe plausible collective patterns, including self-organisation.

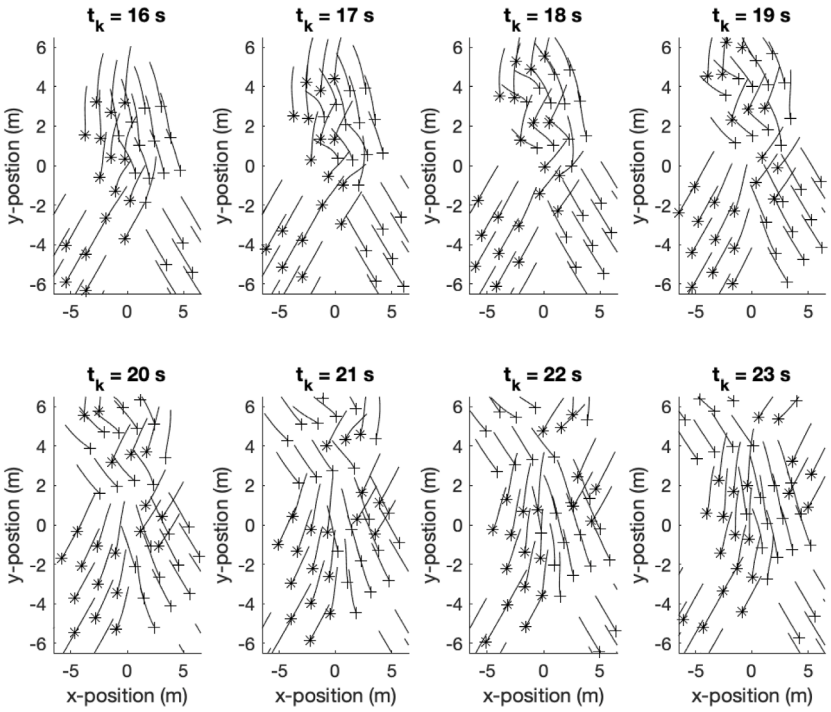

Fig. 13. Example of model behaviour for crossing flow for multiple cyclists for $T = 2.5$ s and $c_{\phi}^{0} = 0.1$.

Future research is aimed at reducing the computational complexity of the model. The game theoretical framework now requires an iterative solution scheme to solve the mixed initial–terminal boundary problem, which is computationally demanding (see Hoogendoorn et al. (2012)).

Furthermore, calibration and validation of the model using real data (e.g those collected during our extensive bicycle experiments Yuan et al. (2018) and Gavriilidou et al. (2019b)) is an important step in making the model of practical use to engineering applications. The comparisons done here provide a first idea on what results we expect (large variety in behaviour, reflected in different parameter values), and will provide empirical evidence on parameter values of dominating strategies. It is clear that for the calibration, the microscopic data stemming from the experiments will be most useful, although relating the parameters to the macroscopic characteristics of the flow (e.g. jam density, capacity, free speed, speed variation, shock wave speeds) will also enable estimation of (some of the) parameters. Microscopic data can be collected in different ways, e.g. using advanced sensor technology, which allows collecting data in the field as well as by controlled experiments.[1] The approach described in Hoogendoorn and Hoogendoorn (2010) can be used as a basis for model identification using different types of data of levels of aggregation. In the validation of the model, special attention is to be paid to the validity under different demand conditions (e.g., dilute or busy conditions). This will reveal the various situations in which the model is applicable.

One of the key issues to investigate is if we can capture the observed heterogeneity in the controlled experiments performed in Yuan et al. (2018) and Gavriilidou et al. (2019b) in a number of (latent) rider classes describing they risk proneness and other characteristics. This will reduce the problem of calibrating the model for any given situation to determining the – possibly context-dependent – composition of the flow with respect to these classes. Next to detailing the calibration methodology, this will be an important future research direction.

CRediT authorship contribution statement

Serge Hoogendoorn: Conceptualization, Methodology, Software, Investigation, Writing - original draft, Writing - review & editing, Funding acquisition. **Alexandra Gavriilidou:** Methodology, Resources, Writing - original draft, Writing - review & editing. **Winnie Daamen:** Writing - review & editing. **Dorine Duives:** Writing - review & editing.

Acknowledgements

This research was supported by the ALLEGRO project, which is financed by the European Research Council (Grant Agreement No. 669792).

[1] We refer to https://www.tudelft.nl/covid/mobiliteit/ for an example of using advanced sensor technology for collecting microscopic field data.

References

Andresen, E., Chraibi, M., Seyfried, A., Huber, F., 2013. Basic driving dynamics of cyclists. In: Simulation of Urban MObility User Conference, pp. 18-32.

Escalona, J.L., Recuero, A.M., 2012. A bicycle model for education in multibody dynamics and real-time interactive simulation. Multibody Syst. Dyn. 27 (3), 383–402.

Gavriilidou, A., Daamen, W., Yuan, Y., Hoogendoorn, S.P., 2019a. Modelling cyclist queue formation using a two-layer framework for operational cycling behaviour. Transp. Res. C 105, 468–484.

Gavriilidou, A., Daamen, Y., Hoogendoorn, S.P., 2021. To yield or not to yield? A behavioural model at unsignalised bicycle crossings. Transp. Res. C (submitted for publication).

Gavriilidou, A., Wierbos, M.J., Daamen, W., Yuan, Y., Knoop, V.L., Hoogendoorn, S.P., 2019b. Large-scale bicycle flow experiment: Setup and implementation. Transp. Res. Rec. 2673 (5), 709–719.

Gavriilidou, A., Yuan, Y., Farah, H., Hoogendoorn, S.P., 2017. Microscopic cycling behaviour model using differential game theory. In: Proceedings of Traffic and Granular Flow 2017.

Guo, N., Jiang, R., Wong, S.C., Hao, Q., Xue, S., Hu, Mao-Bin, 2019. Bicycle flow dynamics on wide roads: Experiment and modeling. arxiv.org..

Helbing, D., Verkehrsdynamik, 1996. Neue Physikalische Modellierungskonzepte. Springer.

Hoogendoorn, S., Bovy, P.H.L., 2003. Simulation of pedestrian flows by optimal control and differential games. Optim. Control Appl. Methods 24 (3), 153–172.

Hoogendoorn, S., Daamen, W., Shu, Y., Ligteringen, H., 2013. Modeling human behavior in vessel maneuver simulation by optimal control and game theory. Transp. Res. Rec. 2326, 45–53.

Hoogendoorn, S., Hoogendoorn, R., 2010. Calibration of microscopic traffic-flow models using multiple data sources. Phil. Trans. R. Soc. A 368 (1928), 4497–4517.

Hoogendoorn, S., Hoogendoorn, R.G., Daamen, W., 2011. Wiedemann revisited: New trajectory filtering technique and its implications for car-following modeling. Transp. Res. Rec. 2260, 152–162.

Hoogendoorn, S., Hoogendoorn, R., Wang, M., Daamen, W., 2012. Modeling driver, driver support, and cooperative systems with dynamic optimal control. Transp. Res. Rec. 2316, 20–30.

Huang, L., Wu, J., You, F., Lv, Z., Song, H., 2017. Cyclist social force model at unsignalized intersections with heterogeneous traffic. IEEE Trans. Ind. Inf. 13 (2), 782–792.

Li, M., Shi, F., Chen, D., 2011. Analyze bicycle-car mixed flow by social force model for collision risk evaluation. In: 3rd International Conference on Road Safety and Simulation, pp. 1-22.

Liang, X., Baohua, M., Qi, X., 2012. Psychological-physical force model for bicycle dynamics. J. Transp. Syst. Eng. Inform. Technol. 12 (2), 91–97.

Ma, X., Luo, D., 2016. Modeling cyclist acceleration process for bicycle traffic simulation using naturalistic data. Transp. Res. F: Traffic Psychol. Behav. 40, 130–144.

Mallikarjuna, C., Rao, K.R., 2009. Cellular automata model for heterogeneous traffic. J. Adv. Transp. 43 (3), 321–345.

Mohammed, Hossameldin, Bigazzi, Alexander Y., Sayed, Tarek, 2019. Characterization of bicycle following and overtaking maneuvers on cycling paths. Transp. Res. C 8, 139–151.

Robin, Th., Antonini, G., Bierlaire, M., Cruz, J., 2009. Specification, estimation and validation of a pedestrian walking behavior model. Transp. Res. B 43 (1), 36–56.

Vasic, J., Ruskin, H.J., 2012. Cellular automata simulation of traffic including cars and bicycles. Physica A 391 (8), 2720–2729.

Yao, D., Zhang, Y., Li, L., Su, Y., Cheng, S., Xu, W., 2009. Behavior modeling and simulation for conflicts in vehicles-bicycles mixed flow. IEEE Intell. Transp. Syst. Mag. 1 (2), 25–30.

Yuan, Y., Goñi-Ros, B., Daamen, W., Hoogendoorn, S.P., 2018. Investigating cyclist interaction behavior through a controlled laboratory experiment. J. Transp. Land Use 11 (1), 833–847.

Zhao, Y., Zhang, H.M., 2017. A unified follow-the-leader model for vehicle, bicycle and pedestrian traffic. Transp. Res. B 105, 315–327.